Acta Tropica 123 (2012) 170–177

Contents lists available at SciVerse ScienceDirect

Acta Tropica

journal homepage: www.elsevier.com/locate/actatropica

Real-time PCR strategy for parasite quantification in blood and tissue samples of experimental *Trypanosoma cruzi* infection

Sérgio Caldas[c,d], Ivo Santana Caldas[c], Lívia de Figueiredo Diniz[c], Wanderson Geraldo de Lima[a,c], Riva de Paula Oliveira[b,c], Alzira Batista Cecílio[d], Isabela Ribeiro[e], André Talvani[a,c], Maria Terezinha Bahia[a,c,*]

[a] *Departamento de Ciências Biológicas, Universidade Federal de Ouro Preto, Campus universitário, Morro do Cruzeiro, Ouro Preto, Minas Gerais, Brazil*
[b] *Departamento de Evolução, Biodiversidade e Meio Ambiente, Universidade Federal de Ouro Preto, Campus universitário, Morro do Cruzeiro, Ouro Preto, Minas Gerais, Brazil*
[c] *Núcleo de Pesquisas em Ciências Biológicas, Universidade Federal de Ouro Preto, Campus universitário, Morro do Cruzeiro, Ouro Preto, Minas Gerais, Brazil*
[d] *Fundação Ezequiel Dias, Rua Conde Pereira Carneiro, 80, Gameleira, Belo Horizonte, Minas Gerais, Brazil*
[e] *Drugs for Neglected Disease Initiative, 1202 Geneve, Switzerland*

ARTICLE INFO

Article history:
Received 28 July 2011
Received in revised form 30 April 2012
Accepted 8 May 2012
Available online 18 May 2012

Keywords:
Trypanosoma cruzi
Real-time PCR
Experimental model
Inflammation
Chemotherapy

ABSTRACT

The lack of an accurate diagnosis has been a serious obstacle to the advancement of the anti-*Trypanosoma cruzi* chemotherapy and long-term infection can result in different health risks to human. PCRs are alternative methods, more sensitive than conventional parasitological techniques, which due to their low sensitivities are considered unsuitable for these purposes. The aim of this study was to investigate a sensitive diagnostic strategy to quantify blood and cardiac tissues parasites based on real-time PCR tools during acute and chronic phases of murine Chagas disease, as well as to monitor the evolution of infection in those mice under specific treatment. In parallel, fresh blood examination, immunological analysis and quantification of cardiac inflammation were also performed to confront and improve real-time PCR data. Similar profiles of parasitemia curves were observed in both quantification techniques during the acute phase of the infection. In contrast, parasites could be quantified only by real-time PCR at 60 and 120 days of infection. In cardiac tissue, real-time PCR detected *T. cruzi* DNA in 100% of infected mice, and using this tool a significant Pearson correlation between parasite load in peripheral blood and in cardiac tissue during acute and chronic phases was observed. Levels of serum CCL2, CCL5 and nitric oxide were coincident with parasite load but focal and diffuse mononuclear infiltrates was observed, even with significant ($p < 0.05$) reduction of parasitism after 60 days of infection. Later, this methodology was used to monitor the evolution of infection in animals treated with itraconazole (Itz). Itz-treatment induced a reduction of parasite load in both blood and cardiac muscle at the treatment period, but after the end of chemotherapy an increase of parasitism was detected. Interestingly, inflammatory mediators levels and heart inflammation intensity had similar evolution to the parasite load, in the group of animals treated. Taken together, our data show that real-time PCR strategy used was suitable for studies of murine *T. cruzi* infection and may prove useful in investigations involving experimental chemotherapy of the disease and the benefits of treatment in relation to parasitism and inflammatory response.

1. Introduction

The American trypanosomiasis or Chagas disease, discovered in 1909 by Carlos Justiniano Ribeiro das Chagas, is a zoonosis caused by the protozoan *Trypanosoma cruzi* (Chagas, 1909). This zoonosis is typical of Latin America extending to the southeastern of the United States of America. Significant advances have taken place in the control of vectorial and transfusional transmission of the disease in some parts of the endemic area, particularly by the Southern Cone initiative that led to interruption of vector-to-human and human-to-human propagation of the disease in Uruguay, Chile and Brazil in recent years (Dias et al., 2002; Schofield et al., 2006). However, due to migrational movements of people from endemic countries, Chagas disease has been reported in non-endemic areas where the congenital transmission, blood transfusion and organ transplant plays an important role (Gascon et al., 2007). Therefore, there are still many challenges to achieve full control

Abbreviations: TNF-α, tumor necrosis factor-alpha; CCL5, regulated upon activation, normal T cell expressed and secreted; CCL2, monocyte chemoattractant protein-1; NO, nitric oxide; FBE, fresh blood examination; d.i., days of infection; Itz, itraconazole.

* Corresponding author at: Laboratório de doença de Chagas, DECBI/NUPEB, Universidade Federal de Ouro Preto, ICEB, Campus Morro do Cruzeiro, 35400-000 Ouro Preto, MG, Brazil. Tel.: +55 31 3559 1690; fax: +55 31 3559 1680.
E-mail address: mtbahia@nupeb.ufop.br (M.T. Bahia).

0001-706X/$ – see front matter © 2012 Elsevier B.V. All rights reserved.
http://dx.doi.org/10.1016/j.actatropica.2012.05.002

or elimination of the disease, mainly due to the uneven progress of the vectorial/transfusional control programs in other parts of the continent, limitations of diagnostic methods and significant limitations of current chemotherapy available (Urbina, 2010).

Chagas disease begins with an acute phase characterized by the presence of parasites in the bloodstream and different tissues of the infected individual. Nonspecific symptoms and myocarditis are common features during the early stage of the infection (Dias, 1992). Infiltration of T cells and macrophages into the heart tissue during the acute phase of the infection is essential for controlling the parasite replication (Hardison et al., 2006). Additionally, cardiac parasitism was apparently related to the increased expression of cytokines and chemokines (Villalta et al., 1998; Talvani et al., 2000), in which the chemokines correlated in the uptake and killing of the intracellular parasites by inducing NO synthase activation enhancing NO production by macrophages and cardiomyocytes (Villalta et al., 1998; Teixeira et al., 2002; Talvani and Teixeira, 2011).

Molecular assays have been widely used for the diagnosis and monitoring of disease progression and therapy outcome in Chagas disease (Moser et al., 1989; Junqueira et al., 1996; Kirchhoff et al., 1996; Marcon et al., 2002). PCRs are alternative methods, more sensitive than conventional parasitological techniques, such as hemoculture, which due to their low sensitivities are considered unsuitable for these purposes (WHO, 2002). For instance, nested-PCR (N-PCR) has demonstrated greater sensitivity than conventional PCR and it has been described as an extremely sensitive method for the diagnosis of Chagas disease (Marcon et al., 2002). However, the disadvantage of this technique is the time required for their achievement and the great risk of false positives results caused by contaminating amplicons (Piron et al., 2007).

In contrast, real-time PCR uses fluorescent dyes or probes allowing the continuous monitoring of the reaction during the amplification process, instead of the amount of target accumulated after a fixed number of cycles. This completely revolutionizes the way to approach the quantification of DNA and RNA. Once the nucleic acid amplification and detection steps are performed in one tube, the risk of releasing amplified nucleic acids to the environment and contamination of subsequent assays is very low compared to the risk conferred by conventional PCR or N-PCR (Cockerill, 2003; Bankowski and Anderson, 2004). Thus, the combination of excellent sensitivity and specificity, low contamination risk and greater speed of work has made the technology of real-time PCR a highly applicable tool, useful for many purposes, such as laboratory diagnostics, gene expression analysis, quantification of parasites and many other applications in the field of research (Duffy et al., 2009; de Freitas et al., 2011). The aim of this study was to standardize an accurate real-time PCR strategy for detection and quantification of *T. cruzi* DNA in the blood and heart of infected mice during the acute phase and chronic disease transition, assessing the correlation between blood and tissue parasitism, inflammatory mediators CCL2, CCL5, nitric oxide and the applicability of this approach to monitor the course of infection during the treatment of mice.

2. Materials and methods

2.1. Parasite and infection

The VL-10 strain of *T. cruzi*, DTU II (Moreno et al., 2010) which is resistant to benznidazole treatment (Filardi and Brener, 1987) has been maintained cryopreserved in liquid nitrogen at Laboratory of Chagas disease, Universidade Federal de Ouro Preto (UFOP), Brazil. Thirty female Swiss mice (age, 3–4 weeks; weight, 18–22 g) were inoculated in groups with 5×10^3 bloodstream forms of *T. cruzi* by intraperitoneal route in a total of two independent experiments. All procedures and experimental protocols were conducted in accordance with the COBEA (Brazilian School of Animal Experimentation) guidelines for the use of animals in research and approved by the Ethics Committee in Animal Research at UFOP (number 2009/17).

2.2. Blood and tissue parasite quantification

Blood parasite quantification were performed at 10, 12, 14, 16, 20, 30, 40, 50, 60, and 120 days after infection (d.i.) ($n = 6$). Two methods were used for measurement of blood parasitism: (i) microscopic fresh blood examination (FBE): 5 μL of blood were collected from the mouse's tail and the number of parasites was estimated as described by Brener (1962). (ii) Real-time PCR: 200 μL of blood was collected from orbital venous sinus of animals and mixed to 35 μL of 129 mM sodium citrate solution (DOLES, BR). The collected material was subjected to DNA extraction. The extracted DNA was frozen at −20 °C until required. In both methods (i) and (ii), curves were plotted using parasitemia average of six mice.

The curves of cardiac parasitism were generated by real-time PCR. We collected 30 mg of heart tissue of animals at 10, 16, 30, 60 and 120 d.i ($n = 6$). This material was stored at −70 °C until DNA extraction. The extracted DNA was frozen at −20 °C for later *T. cruzi* quantification by real-time PCR. Curves were plotted using parasitism average of six mice.

2.3. Treatment schedule

Groups of 24 mice inoculated intraperitoneally with 5×10^3 trypomastigotes were treated with Itraconazole (Itz): 4-[4-[4-[4-[[2-(2,4-dichlorophenyl)-2-(1H-1,2,4-triazol-1-ylmethyl)-1,3-dioxolan-4-yl]methoxy]phenyl]-1-piperazinyl]phenyl]-2,4-dihydro-2-(1-methylpropyl)-3H-1,2,4-Triazol-3-one. Treatments were started on the 10th day after infection and were administered by gavage for 20 consecutive days. Itz were suspended in water with 4% methylcellulose (Sigma) and were administered in doses of 100 mg/kg body weight. This treatment protocol was standardized previously by Toledo et al. (2003).

2.4. DNA preparation and real-time PCR

The extraction of total genomic DNA from blood and tissue of animals infected with *T. cruzi* was performed using the commercial kit (Wizard® Genomic DNA Purification Kit, Promega) with modifications for DNA extraction from cardiac tissue of mouse. The modification consisted in the incubation of 30 mg of sample at 55 °C for 2 h with 120 μL of 0.5 M EDTA solution (pH 8.0) (Sigma®), 500 μL of nucleic lysis solution (Promega) and 9 μL of proteinase K (fungal) (Invitrogen™) at 20 mg/mL followed by maceration and treatment according to the manufacturer's specifications for extraction of tissue DNA. DNA was quantified by spectrophotometer (Pharmacia Biotech Genequant) and the concentrations were adjusted to 25 ng/μL.

The PCR reaction were performed in 10 μL containing 50 ng of genomic DNA, 5 μL of SYBR® Green PCR Mastermix (Applied Biosystems) and either 0.35 μM for *T. cruzi* 195 base pairs (bp) repeat DNA-specific primers or 0.50 μM of murine-specific tumor necrosis factor-α (TNF-α) primers. The primers for *T. cruzi* repetitive DNA (TCZ-F 5′-GCTCTTGCCCACAMGGGTGC-3′, where M = A or C and TCZ R 5′-CCAAGCAGCGGATAGTTCAGG-3′) amplify a 182-bp as described by Cummings and Tarleton (2003). Primers for murine TNF-α (TNF-5241 5′-TCCCTCTCATCAGTTCTATGGCCCA-3′ and TNF-5411 5′-CAGCAAGCATCTATGCACTTAGACCCC-3′) amplify a 170-bp product (Cummings and Tarleton, 2003). The cycling program consisted of an initial denaturation at 95 °C for 10 min, followed by 40 cycles of 94 °C for 15 s and 64.3 °C for 1 min with fluorescence

acquisition at 64.3 °C. Amplification was immediately followed by a melt program with an initial denaturation of 15 s at 95 °C, cooling to 60 °C for 1 min and then a stepwise temperature increase of 0.3 °C/s from 60 to 95 °C.

Each 96-well reaction plate contained standard curve and two negative controls. Negative controls consisted of a reaction with *T. cruzi*-specific or murine-specific primers without DNA and also with blood or tissue DNA from non-infected mice. Each DNA sample was quantified in duplicate. The mean quantification values for *T. cruzi* DNA were normalized by the data obtained with the murine-specific (TNF-α) primers as follows: normalized value = (mean *T. cruzi* DNA/mean TNF-α DNA) × 1000, where "1000" corresponds to the expected value for TNF-α from 200 μL of blood or 30 mg of heart tissue. The efficiencies of amplification were determined automatically by the StepOne™ Software v2.0 by calculating: efficiency $(E) = 10^{(-1/\text{slope})}$ (Stordeur et al., 2002).

2.5. T. cruzi standard calibration curve

Standard curves were generated from five serial dilutions in water (1:10) of DNA extracted from blood and tissue standards containing 5×10^6 parasites/0.1 mL of blood and 10^6 parasites/30 mg of heart tissue, respectively. The limits of detection of parasites were verified by 6 serial dilutions (1:10) of 100 parasite equiv. (from blood and cardiac tissue standards) in DNA (25 ng/μL) from blood and heart tissue of healthy mice. The terms "blood standard" and "tissue standard" refer to DNA extracted from optimized volumes of blood samples and mass of heart tissue specimens from healthy mice spiked with a known quantity of epimastigotes (VL-10 strain). The standards were generated in sufficient quantities for all real-time PCR assays.

2.6. Histopathology and morphometric analysis

For histopathological analysis, experimental mice were sacrificed on days 10, 30 and 120 (6 animals/group/day). Heart tissues were fixed in 10% formalin and embedded in paraffin. Blocks were cut into 4 μm sections and stained by Hematoxylin and Eosin (H&E) for inflammation assessment. Twenty fields from each slide were randomly chosen at 40× magnification performing a total of 1.49×10^6 μm^2 analyzed myocardium area. Images were obtained through a Leica DM 5000 B microcamera (Leica Application Suite, model 2.4.0R1) and processed by the software Leica Qwin V3 image analyzer. The inflammatory process was evaluated by the correlation index between the number of cells observed in myocardium muscle from non-infected and infected animals (Caldas et al., 2008).

2.7. Immunoassays

Immunoassays were performed using plasma from all experimental animals to detect monocyte chemoattractant protein-1 (MCP-1/CCL2) and Regulated upon Activation, normal T-cell expressed and secreted (RANTES/CCL5). Briefly, flat-bottom 96-well microtiter plates (Nunc) were coated with 100 μL/well of the CCL2 and CCL5 specific chemokine monoclonal antibodies (0.2 μg/mL and 2.0 μg/mL, respectively) for 18 h at 4 °C and then washed with PBS buffer (pH 7.4) containing 0.05% Tween 20 (wash buffer). Nonspecific binding sites were blocked with 300 μL/well of 1% BSA in PBS. Plates were rinsed with wash buffer, and 50 μL/well of samples and standards added followed by incubation for 2 h at room temperature. Seven point standard curves using 2-fold serial dilutions with 1% BSA in PBS, and high CCL2 and CCL5 standards of 250 pg/mL and 2000 pg/mL were used, respectively. Plates were then washed and 100 μL/well of the appropriate CCL2 (50 ng/mL) and CCL5 (400 ng/mL) biotinylated detection antibodies diluted in blocking buffer containing 0.05% Tween 20 were added for 1 h at room temperature. Plates were, then, washed and streptavidin–horseradish peroxidase (0.1 μg/mL) was added for 30 min of incubation at room temperature. Finally, plates were washed and 100 μL/well of the substrate solution – 1:1 mixture of color reagent A (H_2O_2) and color reagent B (Tetramethylbenzidine) – was added and after 30 min of a dark incubation at room temperature, the reaction was stopped by 50 μL/well of 1 M H_2SO_4 solution. Plates were read at 450 nm with wavelength correction at 570 nm in a spectrophotometer (Microplate Reader, model 680, BioRad). All samples were assayed in duplicate using DuoSet® ELISA Development System, R and D Systems®, Minneapolis, MN systems.

2.8. Nitric oxide detection

Nitrite levels in the plasma of mice were determined using the Griess reaction as an index of NO production (Vespa et al., 1994). Briefly, 50 μL of plasma from each animal was diluted with 50 μL of water and treated with 15 μL of a mix of NADPH, FAD and nitrate reductase (at concentrations of 1 U/mL – Sigma®). About 18 h after incubation at 37 °C, samples were deproteinated with 10 μL of zinc sulfate (300 g/L – Sigma®) and centrifuged at 2000 × *g* for 5 min. 50 μL of supernatant samples was combined in a flat-bottom 96-well microtiter plates (Nunc) with a 1:1 mixture of 1% sulfanilamide in 2.5% H_3PO_4 and 0.1% naphtylethylenediamide in 2.5% H_3PO_4 (Sigma®). Plates were incubated for 10 min at room temperature, and the absorbance was measured at 550 nm using the automated Microplate Reader, model 680, BioRad. Nitrite concentrations were determined by using a standard curve of sodium nitrite from 125 to 1 μM.

2.9. Statistical analysis

Data were expressed as mean ± standard deviation. Statistical difference for parasitological data among various groups of mice at different days as well as cytokine levels and intensity of inflammation were determined by the nonparametric Tukey's Multiple Comparison Test. Mann–Whitney test was used when two groups of animals were analyzed. Pearson's correlation (r) was also used to evaluate the association of parasitism in blood and heart tissues. Values of $p < 0.05$ were considered significant.

3. Results

3.1. Standard curves and sensitivity of real-time PCR assay

The primary goal of this study was to standardize a strategy based on real-time PCR for a sensitive and reproducible quantification of parasite load in peripheral blood and heart tissue during acute and chronic experimental Chagas disease in mice, as well as its application in the monitoring of experimental chemotherapy. The tissue and blood standards curves were generated from five serial dilutions of DNA from 10^6 parasites/30 mg of heart tissue and 5×10^6 parasites/0.1 mL of blood for the quantification of *T. cruzi* (based on our previous experience with FBE showing maximum parasitemias around 3–4 million parasites per 0.1 mL blood). The TNF-α DNA was assigned as an arbitrary value of 10^3 in both blood and tissue standards. Fig. 1A shows amplification curves of *T. cruzi* and TNF-α DNA in four log dilutions. Fig. 1B shows the standard curves generated from the linear region of each amplification curve. The efficiency (E) and r values for the heart tissue samples were similar. Fig. 1C illustrates typical melting curves observed after amplification of *T. cruzi* and internal control. The temperature of melting (Tm) observed for the parasite was ∼81 °C and for the internal control was ∼79.3 °C in either DNA extracted from blood and heart tissues.

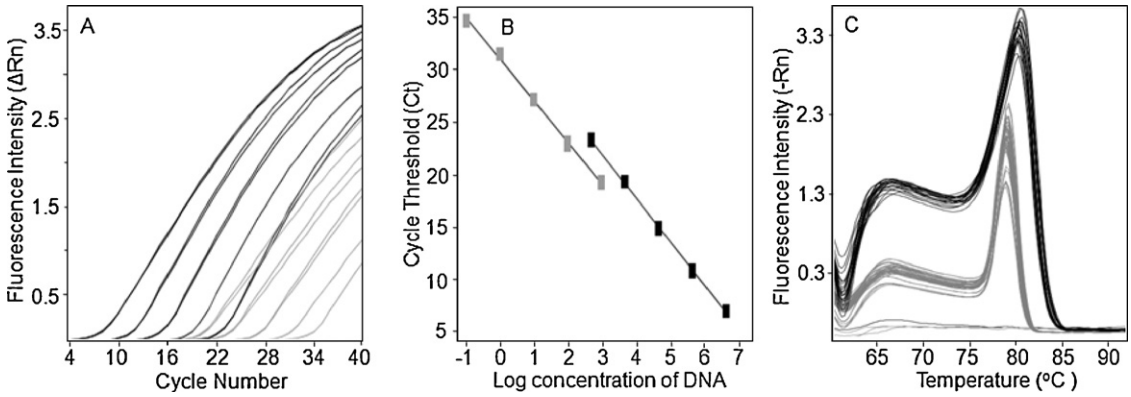

Fig. 1. Standard curve generated with DNA extracted from blood of healthy mice spiked with *Trypanosoma cruzi* epimastigotes (VL-10 strain). The black lines refer to *T. cruzi* DNA and the gray lines to TNF-α DNA (reference gene). (A) Curves were generated with *T. cruzi* and TNF-α primers from five serial dilutions in water (1:10) of DNA extracted from blood standards containing 5×10^6 parasites/0.1 mL of blood. (B) Standard curves were generated from the linear region of each amplification curve. Efficiency of amplification for each primer set was determined using the equation: efficiency (E) = $10^{(-1/\text{slope})}$, being *T. cruzi* E = 93.989% and R^2 = 0.997 and TNF-α E = 93.07% and R^2 = 0.993. (C) Typical melting curves were generated after amplification of *T. cruzi* and TNF-α DNA showing peaks around 81 °C and 79.3 °C, respectively.

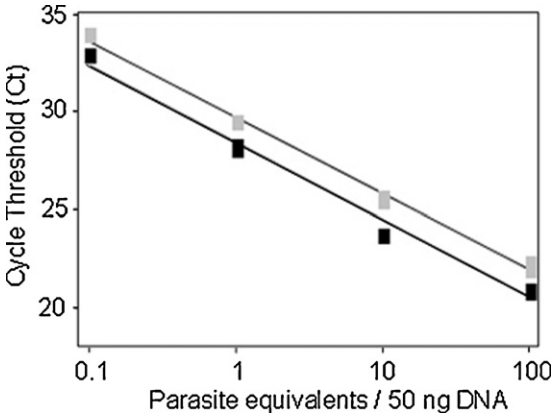

Fig. 2. Limits of detection for both *Trypanosoma cruzi* DNA from blood (gray squares) and heart tissues (black squares) of mice. The limit of detection was 0.1 parasite equiv./50 ng of DNA in both tissues (blood and heart).

Fig. 2 shows the sensitivity of real-time PCR to detect *T. cruzi* DNA from blood and heart tissue of mice. The limits of detection were 0.1 parasite equiv./50 ng DNA. Table 1 represents the reproducibility of two independent tests of real-time PCR with the blood and heart tissues from six mice. The results of the PCR reproducibility were expressed in parasite equiv./50 ng DNA from 0.1 mL of blood and 30 mg of heart tissue.

Table 1
Reproducibility of quantified product from two independent real-time PCR tests performed with the blood and heart tissues from six mice.

Parasite equiv./50 ng DNA Blood sample	Run 1	Run 2	Mean	(S.D.)
1	0.128	0.120	0.124	(0.01)
2	0.520	0.530	0.525	(0.01)
3	0.818	0.825	0.821	(0.01)
4	10.012	9.879	9.946	(0.09)
5	5.082	5.567	5.324	(0.34)
6	3.965	4.081	4.023	(0.08)
Cardiac muscle sample				
1	2.673	2.975	2.824	(0.21)
2	2.272	2.388	2.330	(0.08)
3	1.616	1.651	1.634	(0.02)
4	3.962	4.050	4.006	(0.06)
5	0.927	0.775	0.851	(0.11)
6	3.130	3.057	3.093	(0.05)

3.2. Quantitative analysis of T. cruzi load in blood and cardiac tissues

Next, we assessed the parasite load during the acute and chronic disease transition by real-time PCR and FBE. The parasitemia profiles curves were similar for both quantification techniques during the acute phase of the infection. In contrast, parasites could be quantified only by real-time PCR at a ratio of 159.38 and 174.63 parasites/0.1 mL of blood at 60 and 120 d.i., respectively (Fig. 3). In addition, real-time PCR detected parasite DNA in blood and cardiac tissues in 100% of infected mice in every analysis performed, while FBE showed low and intermittent parasitemia quantification at 40 (16.6%) and 50 (33%) d.i. and negative results at 60 and 120 d.i. as showed in Fig. 4.

In the next, correlations between blood and cardiac tissues parasite burden was evaluated by real-time PCR on days 10, 16, 30, 60 and 120 after infection. During the acute phase of infection parasites were easily detected in both, blood and cardiac tissues, being their burden significantly larger ($p < 0.05$) in blood sample than in cardiac tissue (Fig. 5). Interestingly, after 60 d.i. parasites were more easily detected in cardiac tissue than in peripheral blood.

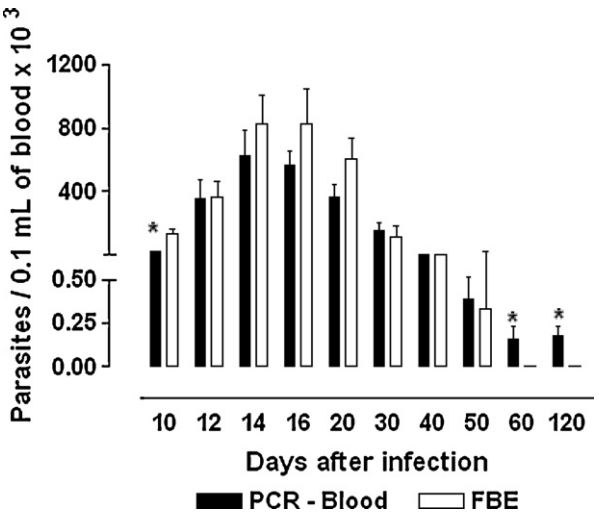

Fig. 3. Average number of parasites detected by real-time PCR (black columns) and fresh blood examination-FBE (white columns) on predetermined days after infection in groups of six mice infected with the VL-10 strain of *T. cruzi*. Data show the averages of two independent experiments. Asterisk denotes a significant difference, as determined by the Mann–Whitney test ($p < 0.05$).

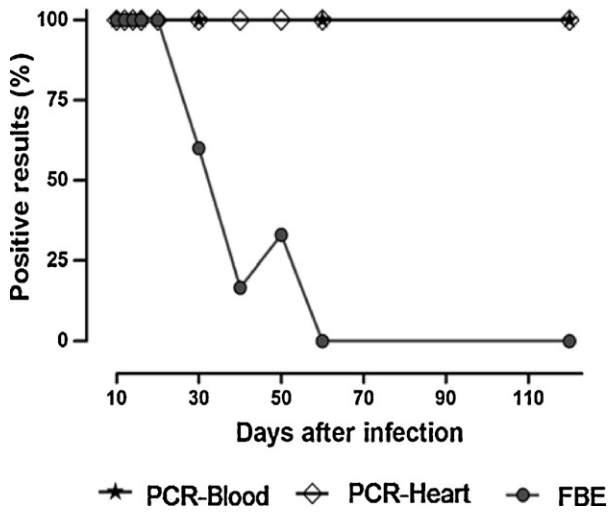

Fig. 4. Percentage of positive results by fresh blood examination (FBE) and real-time PCR in blood (PCR – blood) and heart tissues (PCR – heart) of mice infected with 5×10^3 trypomastigotes of *T. cruzi* (VL-10 strain) at different days after infection. The data represent the average of two independent experiments.

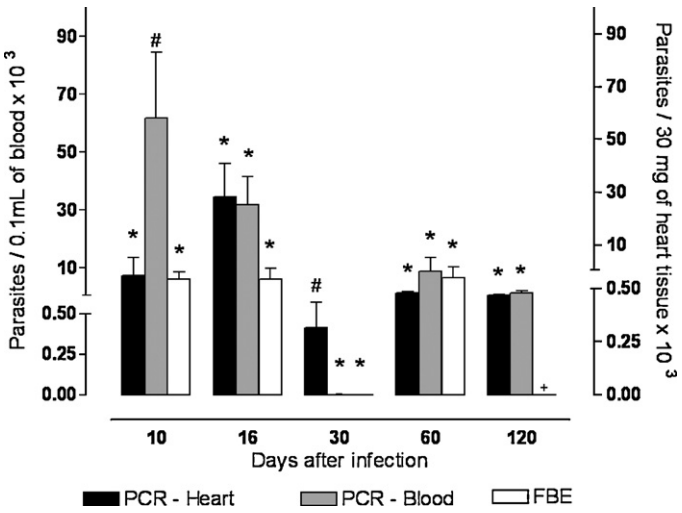

Fig. 6. Parasites detected by Fresh Blood Examination (FBE) and by real-time PCR in blood (PCR – blood) and in cardiac tissues (PCR – heart) of mice inoculated with 5×10^3 trypomastigote forms of *Trypanosoma cruzi* (VL10 strain) and treated with Itraconazole. The treatment was performed on days 10–30 post-infection. Different symbols indicate significant difference ($p < 0.05$).

Considering the results of real-time PCR, the average number of parasites detected in the heart tissue at 60 and 120 d.i. were 2608.83 and 925.31 parasites/30 mg of cardiac tissue and in the peripheral blood were 159.38 and 174.63 parasites/0.1 mL of blood, respectively. There was a significant Pearson correlation between parasite load present in the peripheral blood and in the cardiac tissue during acute and chronic phases of disease ($p < 0.001$ and r value of 0.8068).

Later, in the group of treated animals (Fig. 6), at 30 d.i. (end of chemotherapeutic schedule), the PCR performed with DNA extracted from heart (PCR-H) detected an average of 416.69 parasites/30 mg of heart tissue and the PCR performed with DNA from blood (PCR-B) found an average of 1.16 parasites/0.1 mL of blood. After this period, the levels of parasitism (in blood and heart) increased again, being equivalent at 60 and 120 d.i. by real-time PCR detection. The "+" sign at 120 d.i. indicates a positive result by FBE, detected after exhaustive analysis since the parasite count

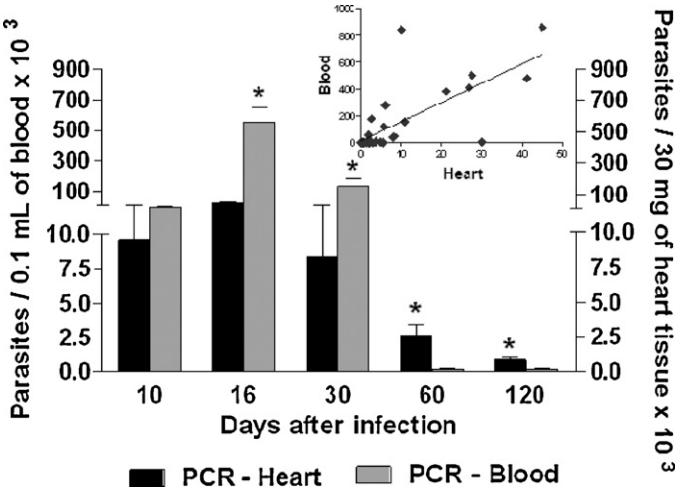

Fig. 5. Blood and heart tissue parasitism detected by real-time PCR in blood (PCR – blood) and heart tissues (PCR – heart) of mice infected with 5×10^3 trypomastigotes of *Trypanosoma cruzi* (strain VL-10) at days 10, 16, 30, 60 and 120 after infection. The data represent the average of two independent experiments. Asterisk denotes a significant difference, as determined by the Mann–Whitney test ($p < 0.05$). The insert represent the correlation analysis of tissue and blood parasitism, being Pearson (r) = 0.8068 and $p < 0.001$.

by the method of Brener (1962) showed negative results. These data showed that the VL-10 strain of *T. cruzi* was fully resistant to Itz, since all treated animals showed parasitism up to 90 days after treatment.

3.3. Immunological analysis and quantification of cardiac inflammation

Correlating with the increasing in parasite burden, serum levels of CCL2 (Fig. 7A) and CCL5 (Fig. 7B) were proportionally elevated during the early acute phase (10 d.i.) of the infection peaking at 30 d.i. with serum levels ~6-fold (CCL2) and ~3-fold (CCL5) higher compared to non-infected mice, except for the treated animals, which showed similar levels to those non-infected animals. However, at the 90 days after treatment, the levels of these chemokines increased and became similar to those non-treated infected animals, which were 3 and 2-fold lowers, respectively, than the levels observed at 30 d.i., but yet higher compared to non-infected mice. Levels of nitric oxide (NO) were also measured in both phases of infection, as showed in Fig. 7C. At 30 d.i. serum concentrations of NO reached ~3.3-fold higher than those observed to healthy mice. Interestingly, when the parasitism was controlled, there was a decrease in NO levels reaching similar levels to healthy animals at 120 d.i., as well as the treated ones, which always had NO levels similar to those non-infected mice.

Besides, at the end of treatment (30 d.i.), treated infected animals (Fig. 8C) showed less inflammatory infiltrate than non-treated infected control (Fig. 8D) but significantly higher ($p < 0.001$) than the healthy mice (Fig. 8B). Furthermore, the partial protection observed after the treatment was not maintained throughout the course of infection (Fig. 8A) and, at 120 d.i., we observed high cellularity in infected animals, regardless of they have been treated or not treated.

4. Discussion

In research laboratories, PCR has been proposed to be an alternative tool for *T. cruzi* quantification since it is more sensitive than the traditional parasitological techniques, such as fresh blood examination, xenodiagnosis and hemoculture (Moser et al., 1989; Junqueira et al., 1996; Kirchhoff et al., 1996; Marcon et al., 2002).

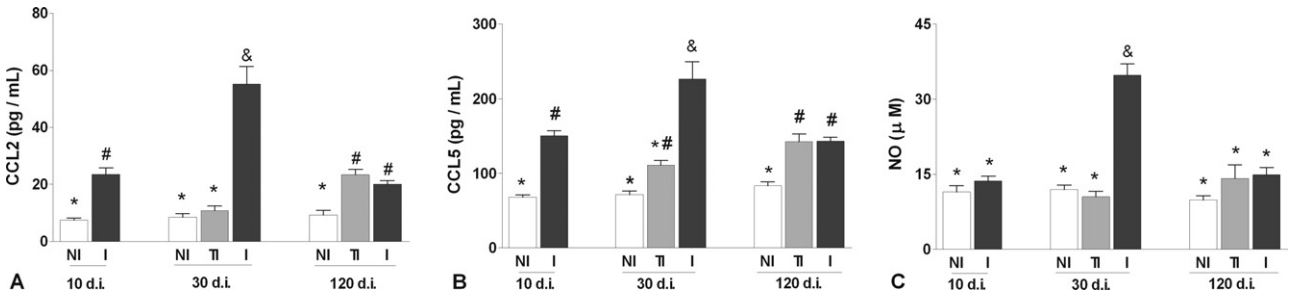

Fig. 7. CCL2 (A), CCL5 (B) and nitric oxide (C) detected in the plasma of mice infected with *T. cruzi* (I), non-infected (NI) and treated infected (TI) at 10, 30 and 120 days of infection (d.i.). Differences were considered significant at $p < 0.05$.

The disadvantage of conventional PCR, however, is time consuming and high risk of false positive results due to carry-over contamination (since the amplified product is detected by gel electrophoresis) along with the impossibility of performing quantitative analysis (Piron et al., 2007), once the calculation of amplified product is limited to the plateau phase of the amplification reaction.

In this context, the quantitative real-time PCR is emerging as an appropriate molecular tool for monitoring parasite load in experimental *T. cruzi* infections. Real-time PCR acquires data at each cycle of the PCR reaction, allowing the calculation of product amount from the log-linear region of the amplification curve (Cummings and Tarleton, 2003). As a target for amplification, satellite *T. cruzi* DNA (represented in 10^4 to 10^5 copies in the parasite genome) highly conserved (Gonzalez et al., 1984; Moser et al., 1989; Elias et al., 2005) was used to provide accurate and efficient PCR based-measurements. Primer set used for *T. cruzi* DNA (Cummings and Tarleton, 2003) is capable of amplifying a tandemly repeated genomic sequence of 195 base pairs (Gonzalez et al., 1984; Moser et al., 1989). The internal control (a single copy of the mouse TNF-α gene) was used to correct variations in initial samples amount, DNA recovery, and samples loading (Cummings and Tarleton, 2003). The optimization of the above mentioned real-time PCR strategy allowed a rapid, reproducible and sensitive quantification of *T. cruzi* directly in blood and heart tissues of mice, as well as monitoring the course of infection in animals under specific treatment. The protocol was followed by confirmation of the amplification specificity by analysis of melting curves.

In this work, PCR inhibitors which can interfere with the amplification cycles and alter the reaction efficiency were minimized with the use of an optimized extraction protocol followed by dilution of the extracted DNA in order to obtain the concentration of 25 ng/μL of DNA. The end point of the curve (100 parasite equiv.) was diluted with 25 ng/μL of DNA to make sure that the high sensitivity observed in the test was not favored by dilution of the standards in water. Thus, it was found that dilution of the standards in water or DNA does not interfere with the test sensitivity. The

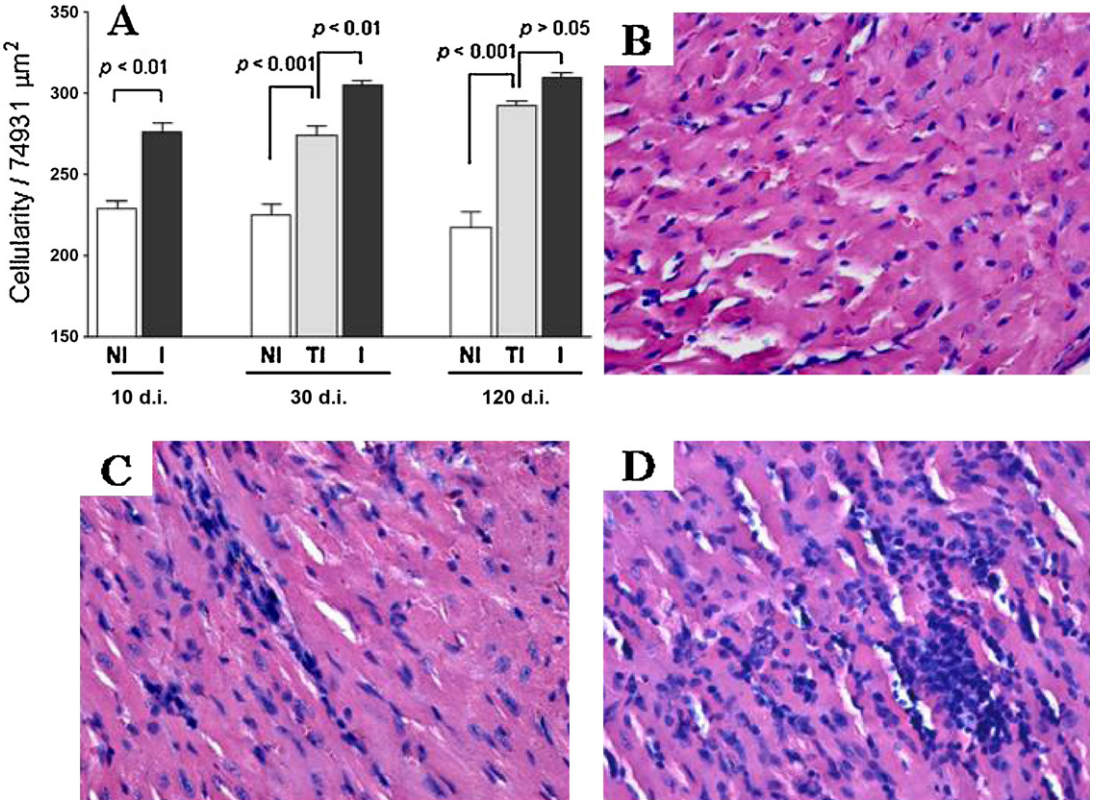

Fig. 8. Analysis of histological sections of hearts from mice infected with VL-10 strain of *Trypanosoma cruzi*. (A) Cellularity of the myocardial sections of mice infected with *T. cruzi* (I), non-infected (NI) and treated infected (TI) at 10, 30 and 120 days of infection (d.i.). Sections of myocardium of NI (B), TI (C) and I (D) at 30 d.i. (*H&E*, 40× *magnification*). Differences were considered significant for $p < 0.05$.

standard curves generated for quantification of blood and tissue parasites showed amplification efficiencies above 90%.

Since the DNA recovery from blood and tissue was significantly variable, it was important to have an internal control to normalize the amount of sample being analyzed in each real-time PCR assay (Cummings and Tarleton, 2003). The DNA of TNF-α present in the standard sample (g enerated with 200 μL of blood or 30 mg of heart tissue) was assigned as an arbitrary value of 10^3, since we do not need to know the absolute value of TNF-α, but the expected value in 200 μL of blood or 30 mg of cardiac tissue to thereby normalize the sample loading errors. The use of a reference gene allowed us to obtain reproducible quantification of *T. cruzi* in blood and heart samples. We demonstrated the reproducibility of the assay by performing the quantification of the same group of blood and heart tissues samples in two PCR tests conducted at different times.

To verify whether the quantification of *T. cruzi* DNA would reflect the number of live parasites present in blood samples, their quantification was always performed in parallel by FBE and real-time PCR. Similar profiles of parasitemia were observed in both methods of quantification; however, the real-time PCR was able to quantify parasites at 60 and 120 d.i. when parasitemia was low. Furthermore, the FBE done in parallel with PCR demonstrates no inhibition and no drugs interference in the PCR quantification of parasitemia.

The standardization of real-time PCR using 200 μL of blood contributed to the higher sensitivity of this technique compared with the FBE, which requires 5 μL of blood (mainly because larger volumes of blood affect the perception and parasites quantification by the observer). However, we cannot disregard the high efficiency of FBE for monitoring the parasitemia during the acute phase of infection and/or when the parasitemia is high. The great advantage of PCR, however, is its application in monitoring of parasites in both blood and cardiac tissue of mice with high sensitivity. At the end of treatment, only the real-time PCR was able to detect and quantify parasitism, as well as during the chronic phase of infection.

Besides, there was a positive correlation between blood and tissue parasitism ($r = 0.8068$ and $p < 0.001$) detected by real-time PCR. Previously, it has also been described a correlation among the parasite burden, the intensity of inflammatory processes and the severity of the disease in both humans and experimental animals (Zhang and Tarleton, 1999; Pérez-Fuentes et al., 2003; Schijman et al., 2004; Benvenuti et al., 2008). Although parasite is the main trigger of cardiac lesions, the immune system of the vertebrate host exerts a decisive role in the development of lesions. The effective immune defense of the vertebrate host requires a flow directed and precise positioning of effectors cells toward the infection site (Luster, 2002). Chemokines such as CCL2 and CCL5, have been observed in human and murine macrophages and cardiomyocytes infected by *T. cruzi* (Villalta et al., 1998; Aliberti et al., 1999; Machado et al., 2000). Several authors have described the role of these chemokines to leukocyte attraction and its likely involvement in controlling the growth of *T. cruzi* and NO production (Sallusto et al., 1998; Villalta et al., 1998; Aliberti et al., 1999; Machado et al., 2000; Coelho et al., 2002; Talvani et al., 2009; Talvani and Teixeira, 2011). Probably the high parasitism in the heart and blood (mainly observed within 30 d.i. in the infected non-treated animals), exerted influence in the increased expression of CCL2 and CCL5 by macrophages and activated $CD4^+$ and $CD8^+$ T cells, contributing to the directed migration of leukocytes to the injury site. According to Paiva et al. (2009), the chemokine CCL2 is produced in large quantities in the heart of mice infected with *T. cruzi* and plays an important role in the destruction of parasites by macrophages. Infected cardiomyocytes coupled to the influx of monocytes/macrophages to the infected heart tissue, probably contribute to the increased production of chemokines and NO. This view also explains the lack of stimulation of these inflammatory molecules in treated animals at 30 d.i. since the parasitism was controlled by the drug at this time. On the other hands, NO, as described by several authors (Saeftel et al., 2001; Machado et al., 2008) exerts trypanocidal activity but also cause damage to infected tissue, which can be aggravated by the influx of $CD8^+$ T cells rich in granulysin and perforin (Stegelmann et al., 2005), directed to the site of infection in a CCL5-dependent manner. However, in parallel with the development of the specific immune response, parasitism levels were controlled and the respective stimulus for the expression of chemokines, cytokines and NO, partially, reduced. Probably this is one reason by which animals have low levels of CCL2, CCL5 and NO at 120 d.i., regardless of whether they were treated or non-treated. But the prevalence of cardiac inflammation at 120 d.i. (in both treated and non-treated mice) suggests an imbalance in the immune response of these animals. Therefore, infection with *T. cruzi* should not be linked invariably to a distinct parasite load, but a fine balance between responses that, although essential for host resistance, may also contribute to immunopathology (Roggero et al., 2002).

Finally, the experimental model of *T. cruzi* infection used in this study in association with real time PCR, as a primary tool, was suitable showing to be useful in investigations involving experimental chemotherapy and inflammatory response. Besides, the combination of high sensitivity and specificity, low contamination risk and greater speed of work confirm the real-time PCR technology as a modern tool to assist in studies involving the course of Chagas' infection in experimental chemotherapy.

Acknowledgments

This work received financial support from the Drugs for Neglected Disease Initiative (DNDi; Geneva, Switzerland), the UBS Optimus Foundation of Switzerland, Rede Mineira de Bioterismo (FAPEMIG), Universidade Federal de Ouro Preto, and research fellowships from Conselho Nacional de Desenvolvimento Científico e Tecnológico (Bahia, M.T. and Talvani, A.), from Fundação de Amparo à Pesquisa do Estado de Minas Gerais (Caldas, S.) and Coordenação de Aperfeiçoamento de Pessoal de Nível Superior (CAPES) (Caldas, I.S.).

References

Aliberti, J.C., Machado, F.S., Souto, J.T., Campanelli, A.P., Teixeira, M.M., Gazzinelli, R.T., Silva, J.S., 1999. Beta-Chemokines enhance parasite uptake and promote nitric oxide-dependent microbiostatic activity in murine inflammatory macrophages infected with *Trypanosoma cruzi*. Infection and Immunity 67, 4819–4826.

Bankowski, M.J., Anderson, S.M., 2004. Real-time nucleic acid amplification in clinical microbiology. Clinical Microbiology News 26, 9–15.

Benvenuti, L.A., Roggerio, A., Freitas, H.F., Mansur, A.J., Fiorelli, A., Higuchi, M.L., 2008. Chronic American trypanosomiasis: parasite persistence in endomyocardial biopsies is associated with high-grade myocarditis. Annals of Tropical Medicine and Parasitology 102, 481–487.

Brener, Z., 1962. Therapeutic activity and criterion of cure on mice experimentally infected with *Trypanosoma cruzi*. Revista do Instituto de Medicina Tropical de Sao Paulo 4, 389–396.

Caldas, I.S., Talvani, A., Caldas, S., Carneiro, C.M., Lana, M., Guedes, P.M.M., Bahia, M.T., 2008. Benznidazole therapy during acute phase of Chagas disease reduces parasite load but does not prevent chronic cardiac lesions. Parasitology Research 103, 413–421.

Chagas, C., 1909. Nova tripanosomíase humana: estudos sobre a morfologia e o ciclo evolutivo do *Schizotrypanum cruzi* n. gen. n.sp., agente etiológico de nova entidade mórbida do homem. Memorias do Instituto Oswaldo Cruz 1, 159–218.

Cockerill, F.R., 2003. Application of rapid-cycle real-time polymerase chain reaction for diagnostic testing in the clinical microbiology laboratory. Archives of Pathology and Laboratory Medicine 127, 1112–1120.

Coelho, P.S., Klein, A., Talvani, A., Coutinho, S.F., Takeuchi, O., Akira, S., Silva, J.S., Canizzaro, H., Gazzinelli, R.T., Teixeira, M.M., 2002. Glycosylphosphatidylinositol-anchored mucin-like glycoproteins isolated from *Trypanosoma cruzi* trypomastigotes induce *in vivo* leukocyte recruitment dependent on MCP-1 production by IFN-gamma-primed-macrophages. Journal of Leukocyte Biology 71, 837–844.

Cummings, K.L., Tarleton, R.L., 2003. Rapid quantitation of *Trypanosoma cruzi* in host tissue by real-time PCR. Molecular and Biochemical Parasitology 129, 53–59.

de Freitas, V.L., da Silva, S.C., Sartori, A.M., Bezerra, R.C., Westphalen, E.V., Molina, T.D., Teixeira, A.R., Ibrahim, K.Y., Shikanai-Yasuda, M.A., 2011. Real-time PCR in HIV/*Trypanosoma cruzi* coinfection with and without Chagas disease reactivation: association with HIV viral load and CD4 level. PLoS Neglected Tropical Diseases 5, e1277.

Dias, J.C., 1992. Epidemiology of Chagas disease. In: Wendel, S., Brener, Z., Camargo, M.S., Rassi, A. (Eds.), Chagas disease (American Trypanosomiasis): its impact on transfusion and clinical medicine. ISBT Brasil, São Paulo, pp. 49–80.

Dias, J.C., Silveira, A.C., Schofield, C.J., 2002. The impact of Chagas disease control in Latin America: a review. Memorias do Instituto Oswaldo Cruz 97, 603–612.

Duffy, T., Bisio, M., Altcheh, J., Burgos, J.M., Diez, M., Levin, M.J., Favaloro, R.R., Freilij, H., Schijman, A.G., 2009. Accurate real-time PCR strategy for monitoring bloodstream parasitic loads in chagas disease patients. PLoS Neglected Tropical Diseases 3, e419.

Elias, M.C., Vargas, N., Tomazi, L., Pedroso, A., Zingales, B., Schenkman, S., Briones, M.R., 2005. Comparative analysis of genomic sequences suggests that *Trypanosoma cruzi* CL Brener contains two sets of non-intercalated repeats of satellite DNA that correspond to *T. cruzi* I and *T. cruzi* II types. Molecular and Biochemical Parasitology 140, 221–227.

Filardi, L.S., Brener, Z., 1987. Susceptibility and natural resistance of *Trypanosoma cruzi* strains to drugs used clinically in Chagas disease. Transactions of the Royal Society of Tropical Medicine and Hygiene 81, 755–759.

Gascon, J., Albajar, P., Canas, E., Flores, M., Prat, J., Herrera, R.N., Lafuente, C.A., Luciardi, H.L., Moncayo, A., Molina, L., Munoz, J., Puente, S., Sanz, G., Trevino, B., Sergio-Salles, X., 2007. Diagnosis, management and treatment of chronic Chagas' heart disease in areas where *Trypanosoma cruzi* infection is not endemic. Revista Espanola de Cardiologia 60, 285–293.

Gonzalez, A., Prediger, E., Huecas, M.E., Nogueira, N., Lizardi, P.M., 1984. Minichromosomal repetitive DNA in *Trypanosoma cruzi*: its use in a high-sensitivity parasite detection assay. Proceedings of the National Academy of Sciences of the United States of America 81, 3356–3360.

Hardison, J.L., Wrightsman, R.A., Carpenter, P.M., Kuziel, W.A., Lane, T.E., Manning, J.E., 2006. The CC chemokine receptor 5 is important in control of parasite replication and acute cardiac inflammation following infection with *Trypanosoma cruzi*. Infection and Immunity 74, 135–143.

Junqueira, A.C., Chiari, E., Wincker, P., 1996. Comparison of the polymerase chain reaction with two classical parasitological methods for the diagnosis of Chagas disease in an endemic region of north-eastern Brazil. Transactions of the Royal Society of Tropical Medicine and Hygiene 90, 129–132.

Kirchhoff, L.V., Votava, J.R., Ochs, D.E., Moser, D.R., 1996. Comparison of PCR and microscopic methods for detecting *Trypanosoma cruzi*. Journal of Clinical Microbiology 34, 1171–1175.

Luster, A.D., 2002. The role of chemokines in linking innate and adaptive immunity. Current Opinion in Immunology 14, 129–135.

Machado, F.S., Martins, G.A., Aliberti, J.C., Mestriner, F.L., Cunha, F.Q., Silva, J.S., 2000. Trypanosoma cruzi-infected cardiomyocytes produce chemokines and cytokines that trigger potent nitric oxide-dependent trypanocidal activity. Circulation 102, 3003–3008.

Machado, F.S., Souto, J.T., Rossi, M.A., Esper, L., Tanowitz, H.B., Aliberti, J., Silva, J.S., 2008. Nitric oxide synthase-2 modulates chemokine production by *Trypanosoma cruzi*-infected cardiac myocytes. Microbes and Infection 10, 1558–1566.

Marcon, G.E., Andrade, P.D., de Albuquerque, D.M., Wanderley, J.S., de Almeida, E.A., Guariento, M.E., Costa, S.C., 2002. Use of a nested polymerase chain reaction (N-PCR) to detect *Trypanosoma cruzi* in blood samples from chronic chagasic patients and patients with doubtful serologies. Diagnostic Microbiology and Infectious Disease 43, 39–43.

Moreno, M., D'avila, D.A., Silva, M.N., Galvão, L.M., Macedo, A.M., Chiari, E., Gontijo, E.D., Zingales, B., 2010. Trypanosoma cruzi benznidazole susceptibility *in vitro* does not predict the therapeutic outcome of human Chagas disease. Memorias do Instituto Oswaldo Cruz 105, 918–924.

Moser, D.R., Kirchhoff, L.V., Donelson, J.E., 1989. Detection of *Trypanosoma cruzi* by DNA amplification using the polymerase chain reaction. Journal of Clinical Microbiology 27, 1477–1482.

Paiva, C.N., Figueiredo, R.T., Kroll-Palhares, K., Silva, A.A., Silverio, J.C., Gibaldi, D., Pyrrho, A.S., Benjamim, C.F., Lannes-Vieira, J., Bozza, M.T., 2009. CCL2/MCP-1 controls parasite burden, cell infiltration, and mononuclear activation during acute *Trypanosoma cruzi* infection. Journal of Leukocyte Biology 86, 1239–1246.

Pérez-Fuentes, R., Guégan, J.F., Barnabé, C., López-Colombo, A., Salgado-Rosas, H., Torres-Rasgado, E., Briones, B., Romero-Díaz, M., Ramos-Jiménez, J., Sánchez-Guillén, M.C., 2003. Severity of chronic Chagas disease is associated with cytokine/antioxidant imbalance in chronically infected individuals. International Journal for Parasitology 33, 293–299.

Piron, M., Fisa, R., Casamitjana, N., Lopez-Chejade, P., Puig, L., Verges, M., Gascon, J., Prat, J., Portus, M., Sauleda, S., 2007. Development of a real-time PCR assay for *Trypanosoma cruzi* detection in blood samples. Acta Tropica 103, 195–200.

Roggero, E., Perez, A., Tamae-Kakazu, M., Piazzon, I., Nepomnaschy, I., Wietzerbin, J., Serra, E., Revelli, S., Bottasso, O., 2002. Differential susceptibility to acute *Trypanosoma cruzi* infection in BALB/c and C57BL/6 mice is not associated with a distinct parasite load but cytokine abnormalities. Clinical and Experimental Immunology 128, 421–428.

Saeftel, M., Fleischer, B., Hoerauf, A., 2001. Stage-dependent role of nitric oxide in control of *Trypanosoma cruzi* infection. Infection and Immunity 69, 2252–2259.

Sallusto, F., Lanzavecchia, A., Mackay, C.R., 1998. Chemokines and chemokine receptors in T-cell priming and Th1/Th2-mediated responses. Immunology Today 19, 568–574.

Schijman, A.G., Vigliano, C.A., Viotti, R.J., Burgos, J.M., Brandariz, S., Lococo, B.E., Leze, M.I., Armenti, H.A., Levin, M.J., 2004. Trypanosoma cruzi DNA in cardiac lesions of Argentinean patients with end-stage chronic chagas heart disease. American Journal of Tropical Medicine and Hygiene 70, 210–220.

Schofield, C.J., Jannin, J., Salvatella, R., 2006. The future of Chagas disease control. Trends in Parasitology 22, 583–588.

Stegelmann, F., Bastian, M., Swoboda, K., Bhat, R., Kiessler, V., Krensky, A.M., Roellinghoff, M., Modlin, R.L., Stenger, S., 2005. Coordinate expression of CC chemokine ligand 5, granulysin, and perforin in CD8+ T cells provides a host defense mechanism against *Mycobacterium tuberculosis*. Journal of Immunology 175, 7474–7483.

Stordeur, P., Poulin, L.F., Craciun, L., Zhou, L., Schandené, L., de Lavareille, A., Goriely, S., Goldman, M., 2002. Cytokine mRNA quantification by real-time PCR. Journal of Immunological Methods 259, 55–64.

Talvani, A., Coutinho, S.F., Barcelos, L.S., Teixeira, M.M., 2009. Cyclic AMP decreases the production of NO and CCL2 by macrophages stimulated with *Trypanosoma cruzi* GPI-mucins. Parasitology Research 104, 1141–1148.

Talvani, A., Ribeiro, C.S., Aliberti, J.C., Michailowsky, V., Santos, P.V., Murta, S.M., Romanha, A.J., Almeida, I.C., Farber, J., Lannes-Vieira, J., Silva, J.S., Gazzinelli, R.T., 2000. Kinetics of cytokine gene expression in experimental chagasic cardiomyopathy: tissue parasitism and endogenous IFN-gamma as important determinants of chemokine mRNA expression during infection with *Trypanosoma cruzi*. Microbes and Infection 2, 851–866.

Talvani, A., Teixeira, M.M., 2011. Inflammation and Chagas disease: some mechanisms and relevance. Advances in Parasitology 76, 171–194.

Teixeira, M.M., Gazzinelli, R.T., Silva, J.S., 2002. Chemokines, inflammation and *Trypanosoma cruzi* infection. Trends in Parasitology 18, 262–265.

Toledo, M.J., Bahia, M.T., Carneiro, C.M., martins-filho, O.A., Tibayrenc, M., Barnabé, C., Tafuri, W.L., Lana, M., 2003. Chemotherapy with benznidazole and itraconazole for mice infected with different *Trypanosoma cruzi* clonal genotypes. Antimicrobial Agents and Chemotherapy 47, 223–230.

Urbina, J.A., 2010. Specific chemotherapy of Chagas disease: relevance, current limitations and new approaches. Acta Tropica 115, 55–68.

Vespa, G.N., Cunha, F.Q., Silva, J.S., 1994. Nitric oxide is involved in control of *Trypanosoma cruzi*-induced parasitemia and directly kills the parasite *in vitro*. Infection and Immunity 62, 5177–5182.

Villalta, F., Zhang, Y., Bibb, K.E., Kappes, J.C., Lima, M.F., 1998. The cysteine-cysteine family of chemokines RANTES, MIP-1alpha, and MIP-1beta induce trypanocidal activity in human macrophages via nitric oxide. Infection and Immunity 66, 4690–4695.

World Health Organization (WHO), 2002. Control of Chagas disease. Second Report of the WHO Expert Committee. WHO Technical Report Series. 905, Geneva, 109p.

Zhang, L., Tarleton, R.L., 1999. Parasite persistence correlates with disease severity and localization in chronic Chagas' disease. Journal of Infectious Diseases 180, 480–486.